RESEARCH PAPER

BJP · BRITISH PHARMACOLOGICAL SOCIETY

Meprin-α (Mep1A) enhances TNF-α secretion by mast cells and aggravates abdominal aortic aneurysms

Ran Gao[1] | Duan Liu[2] | Wenjun Guo[1] | Weipeng Ge[1] | Tianfei Fan[1] |
Bolun Li[1] | Pan Gao[3] | Bin Liu[4] | Yuehong Zheng[2] | Jing Wang[1] ⓘ

[1]State Key Laboratory of Medical Molecular Biology, Institute of Basic Medical Sciences, Chinese Academy of Medical Sciences, Department of Pathophysiology, Peking Union Medical College, Beijing, China

[2]Peking Union Medical College Hospital, Beijing, China

[3]Department of Geriatrics, Southwest Hospital, The First Affiliated Hospital to Army Medical University, Chongqing, China

[4]Aab Cardiovascular Research Institute, University of Rochester, Rochester, USA

Correspondence
Yuehong Zheng, Peking Union Medical College Hospital, Beijing, China.
Email: yuehongzheng@yahoo.com

Jing Wang, State Key Laboratory of Medical Molecular Biology, Institute of Basic Medical Sciences, Chinese Academy of Medical Sciences, Department of Pathophysiology, Peking Union Medical College, Beijing, China.
Email: wangjing@ibms.pumc.edu.cn

Background and Purpose: Abdominal aorticaneurysm (AAA) rupture is mainly due to elastic lamina degradation. As a metalloendopeptidase, meprin-α (Mep1A) critically modulates the activity of proteins and inflammatory cytokines in various diseases. Here, we sought to investigate the functional role of Mep1A in AAA formation and rupture.

Experimental Approach: AAA tissues were detected by using real-time PCR (RT-PCR), western blotting (WB), and immunohistochemistry. Further mechanistic studies used RT-PCR, WB, and enzyme-linked immunosorbent assays.

Key Results: Mep1A mediated AAA formation by regulating the mast cell (MC) secretion of TNF-α, which promoted matrix metalloproteinase (MMP) expression and apoptosis in smooth muscle cells (SMCs). Importantly, increased Mep1A expression was found in human AAA tissues and in angiotensin II-induced mouse AAA tissues. Mep1A deficiency reduced AAA formation and increased the survival rate of AAA mice. Pathological analysis showed that Mep1A deletion decreased elastic lamina degradation and SMC apoptosis in AAA tissues. Furthermore, Mep1A was expressed mainly in MCs, wherein it mediated TNF-α expression. Mep1A inhibitor actinonin significantly inhibited TNF-α secretion in MCs. TNF-α secreted by MCs enhanced MMP2 expression in SMCs and promoted SMC apoptosis.

Conclusion and Implications: Taken together, these data suggest that Mep1A may be vital in AAA pathophysiology by regulating TNF-α production by MCs. Knocking out Mep1A significantly decreased AAA diameter and improved AAA stability in mice. Therefore, Mep1A is a potential new therapeutic target in the development of AAA.

1 | INTRODUCTION

Abdominal aortic aneurysm (AAA) is the permanent dilation of aorta, which is a major cause of sudden death in the senior population (Jones et al., 2017) and its pathophysiologic characteristics include immune responses (Jalalzadeh et al., 2016), cell apoptosis (Li, Krishna, & Golledge, 2016), extracellular matrix (ECM) degradation (Lindberg, Zarrouk, Holst, & Gottsater, 2016), neovascularization of

---

Abbreviations: Mep1A, meprin-α; Ang II, angiotensin II; AAA, abdominal aortic aneurysm; SMC, smooth muscle cell; MC, mast cell; EC, endothelial cell; ECM, extracellular matrix; MMP, matrix metalloproteinase.

Ran Gao, Duan Liu, Jing Wang, and Yuehong Zheng contributed equally to this work.

the media and adventitia (Sun et al., 2007) and vascular remodelling (Sun et al., 2007). It is diagnosed if the abdominal aorta is dilated to 1.5 times larger than normal (Sakalihasan, Limet, & Defawe, 2005). The risk factors for abdominal aortic aneurysm include being a male of advanced age, atherosclerosis, hypertension and genetic predisposition. Although many theories have been proposed to explain the development of abdominal aortic aneurysm, the pathophysiologic mechanisms underlying abdominal aortic aneurysm progression at the molecular level have not been thoroughly investigated and, to date, there are no effective drugs for preventative treatment (Jones et al., 2017).

Chronic inflammation of the aortic wall, in which mast cell (MC) infiltration plays an important role, is one of the vital pathophysiological mechanisms of abdominal aortic aneurysm formation (Wang et al., 2014). Mast cells release a wide spectrum of cytokines, including IL-1β, IL-6, TNF-α, IFN-γ, TGF-β and osteopontin, which induce matrix metalloproteinase activity, endothelial cell degradation and phenotypic changes in smooth muscle cells (SMCs), leading to abdominal aortic aneurysm formation (Shi & Lindholt, 2013; Tsuruda et al., 2008). Our previous study showed that IgE, a well-known mast cell activator, is highly expressed in abdominal aortic aneurysm tissues. IgE receptor deficiency significantly decreased abdominal aortic aneurysm formation by modulating mast cell function (Wang et al., 2014).

As a member of the astacin family, meprins are associated with the development of inflammation and cancer in the kidneys and intestines (Banerjee et al., 2009; Jefferson et al., 2013). Their substrates are extensive, including endothelial cell proteins and bioactive peptides, both on vascular walls and in peripheral blood. Meprins can hydrolyse, activate or inactivate several cytokines, vasoactive peptides, growth factors and endothelial cell proteins (Jefferson et al., 2013). Therefore, meprins in arterial walls can reduce the concentrations of vasoactive peptides by metabolizing them and can promote inflammation by locally activating inflammatory cytokines, eventually accelerating endothelial cell degradation and promoting vascular remodelling (Gao et al., 2009; Jefferson et al., 2013). Meprin is composed of two subunits, meprin-α (Mep1A) and meprin-β (Mep1B), which form homodimers and heterodimers by forming disulphide bridges. Mep1A is a heterogeneous multimer (Bertenshaw, Norcum, & Bond, 2003) that is expressed ubiquitously in both humans and mice, especially in the intestinal brush border membrane, kidneys, leukocytes and some cancer cells (Jefferson et al., 2013). In atherosclerosis, Mep1A can induce inflammatory cytokine secretion (Gao et al., 2009); thus, Mep1A inhibition may attenuate arterial wall inflammation.

Mep1A has been shown to enhance atherosclerotic plaque formation in peripheral arteries by regulating inflammatory factors in vivo and in vitro (Gao et al., 2009; Gao & Si, 2010; Jefferson et al., 2013). Considering the similar inflammatory pathogenesis of atherosclerosis and abdominal aortic aneurysm, and the ubiquitous expression of Mep1A in various inflammatory sites, this study was performed to investigate the effect of Mep1A on the development of abdominal aortic aneurysm.

What is already known
- Mep1A aggravates atherosclerosis by regulating inflammation.

What this study adds
- Mep1A promoted the occurrence abdominal aortic aneurysms by regulating mast cell secretion of TNF-α.

What is the clinical significance
- Mep1A inhibitor actinonin significantly inhibited TNF-α secretion in mast cell.
- Mep1A may be a potential novel target for alleviating the progression of abdominal aortic aneurysms.

---

2 | METHODS

2.1 | Animal models

To generate ApoE$^{-/-}$Mep1A$^{-/-}$ (KO) mice, ApoE$^{-/-}$ mice (C57BL/6, Beijing Vital River Laboratory Animal Technology Co., Ltd, China) were crossbred with Mep1A$^{-/-}$ mice (C57BL/6, N5, Biocytogen, China). ApoE$^{-/-}$Mep1A$^{+/+}$ (WT) littermates were used as controls.

Mice were weighed and systolic and diastolic BPs were measured using the CODA$^{®}$ non-invasive BP system (Kent Scientific Co., Torrington, CT) before and after abdominal aortic aneurysm modelling. To induce abdominal aortic aneurysm, 9-week-old male mice were implanted with osmotic pumps (Alzet MODEL 2004; DURECT, Cupertino, CA) that released angiotensin II (Ang II; 1,000 ng·kg^{-1}·min^{-1}; Sigma, Cat#: A9525-50MG) for 28 days, as described previously (Daugherty, Manning, & Cassis, 2000). Based on previous experience and published data (Daugherty et al., 2000; Li et al., 2018) and considering the high mortality of Ang II-treated WT mice, four groups of mice were used as follows:- WT mice treated with PBS (n = 5), KO mice treated with PBS (n = 6), WT mice treated with Ang II (n = 22) and KO mice treated with Ang II (n = 12). The Ethics Committee of Peking Union Medical College approved the study protocol. Animal studies are reported in compliance with the ARRIVE guidelines (Kilkenny et al., 2010; McGrath & Lilley, 2015) and with the recommendations made by the *British Journal of Pharmacology*. The experimenter performing the behavioural testing was blind to the genotype and treatment.

2.2 | Human aortic tissue

Human aortic tissue extracts were prepared from six abdominal aortic aneurysm patients (Peking Union Medical College Hospital and Fuwai Hospital) and from the bodies of seven deceased donors with no detectable vascular disease (Peking Union Medical College Volunteer

Corpse Donation Reception Station). The clinical information associated with the samples is shown in Table S1. The human aortic tissues obtained were approved by the Human Investigation Review Committee at Peking Union Medical College.

2.3 | Immunohistochemical and immunofluorescence analysis

Human aortic aneurysm tissues were immediately embedded in optimal cutting temperature compound and stored at $-80°C$. Immunohistochemistry with rabbit anti-human and anti-mouse Mep1A antibodies (1:100, Invitrogen, Cat#: PA5-96943) was performed on acetone-fixed frozen sections of human abdominal aortic aneurysm tissue and control normal aortas by the 3-amino-9-ethylcarbazole method.

Mouse aorta segments were cut at the maximal suprarenal outer aortic diameter and embedded vertically with optimal cutting temperature compound. Ten to fifteen serial frozen sections covering the maximal dilated aorta were prepared as described previously (Schulte et al., 2010; Zhang et al., 2012). Slides of each sample from identical levels were stained with each antibody. Serial cryostat cross sections (6 μm) were stained for Mep1A (1:100; Invitrogen, Cat#: PA5-96943), elastin (Modified Verhoeff Van Gieson Elastic Stain Kit, Sigma, Cat#: HT25A), matrix metalloproteinase 2 (1:100; Abcam, Cat#: ab86607), Collagen I (1:100; Proteintech, Cat#: 14695-1-AP), tryptase (1:100; Abcam, Cat#: ab2378), Mac-3 (macrophage marker, 1:2,000; Abcam, Cat#: ab203224), major histocompatibility complex (MHC)-II (1:250; Abcam, Cat#: ab180779), CD4^{+} (T cell marker, 1:90; Abcam, Cat#: ab185685), TNF-α (1:100; Abcam, Cat#: ab6671) and TUNEL (Roche Diagnostics, USA, Cat#: 11684817910). The relative contents of Mep1A, TNF-α, matrix metalloproteinase 2 and Collagen I within the aortas were quantified by measuring the positively stained area using computer-assisted image analysis software (Image-Pro Plus; Media Cybernetics, Bethesda, MD, RRID:SCR_007369). CD4^{+} T cells, macrophages, MHC-II-positive antigen-presenting cells and tryptase-positive mast cells were quantified as the number of cells per square millimetre. Five mice were randomly selected for immunohistochemical analysis from each group. For each mouse, three sections from the maximal diameter of vessel were stained and quantified. The percentage of positive area (%) was defined as the ratio of positive red staining area to the total vascular area. The value obtained from 15 sections were averaged and statistics analysis was performed. Negative staining controls (without primary antibodies) were shown in Figure S1A,B. Elastin degradation was graded according to the key provided by the manufacturer (Deckert et al., 2013).

Immunofluorescence staining of Mep1A and tryptase proteins was performed using rabbit anti-Mep1A (1:100; Invitrogen, Cat#: PA5-96943), mouse anti-tryptase (1:100; Abcam, Cat#: ab2378), mouse anti-CD31(1:30, Santa Cruz, Cat#: sc-376764), mouse anti-α smooth muscle actin (1:100; Abcam, Cat#:ab7817), FITC-conjugated

goat anti-mouse IgG (1:1,000, Invitrogen, Cat#: F-2761, RRID: AB_2536524) and PE-conjugated goat anti-rabbit IgG (1:1,000, Invitrogen, Cat#: P-2771MP, RRID:AB_221651) on acetone-fixed frozen sections of human abdominal aortic aneurysm tissue. The immuno-related procedures used comply with the recommendations made by the *British Journal of Pharmacology* (Alexander et al., 2018).

2.4 | Real-time PCR

Total RNA was extracted from abdominal aortic aneurysm tissues or cells using TRIzol reagent (Invitrogen, Carlsbad, CA, Cat#: 15596018). The RNA samples were then treated with RNase-free DNase (Thermo, Carlsbad, CA, Cat#: EN0521) to remove genomic DNA contamination. Equal amounts of RNA were reverse transcribed, and quantitative PCR was performed in a single-colour RT-PCR detection system (Bio-Rad, Hercules, CA, USA). The mRNA levels of TNF-α, IL-1β, matrix metalloproteinase 2, Collagen I, Mep1A and Mep1B were normalized to the level of the housekeeping gene GAPDH. The RT-PCR primers are shown in Table S2.

2.5 | Western blot analysis and zymography

Protein was extracted from aortic tissues or cells in lysis buffer containing 50-mM Tris–HCl (pH 7.4), 150-mM NaCl, 1-mM EDTA, 10% glycerol, 1% Triton X-100, and a protease and phosphatase inhibitor cocktail (Thermo Scientific, Cat#: 78447). The protein concentration was measured using a BCA kit (Pierce, Holmdel, NJ, US, Cat#: 23225). Equal amounts of protein extracts (30 μg per lane) were separated by 8% or 12% SDS-PAGE and transferred to a PVDF membrane, which was probed with Mep1A polyclonal antibodies (1:1,000, Invitrogen, Cat#: PA5-96943), Mep1B antibody (1:1,000, Abcam, ab42743, RRID:AB_2143453), matrix metalloproteinase 2 antibody (1:1,000, Abcam, Cat#: ab86607, RRID:AB_10672798) and Collagen I antibody (1:1,000, Proteintech, Cat#: 14695-1-AP). Immunoblotting of the housekeeping protein GAPDH (1:5,000, Proteintech, Cat#: 60004-1-Ig) or α-tubulin (1:200, Santa Cruz Biotechnology, Cat#: sc-69969) was performed to ensure equal protein loading. After three washes with TBST, the membrane was incubated with an HRP-labelled rabbit or mouse secondary antibody (Invitrogen, 1:5,000 or 1:4,000) for 1 hr at room temperature. Immunoreactive bands were visualized with SuperSignal™ West Pico PLUS Chemiluminescent Substrate (Pierce, Cat#: 34577). In this study, western blotting has been conducted. The experimental detail provided conforms with BJP Guidelines (Alexander et al., 2018). Matrix metalloproteinase 2 activity was detected by Zymography using a matrix metalloproteinase kit (Shanghai Xin Fan Biotechnology Co. CA, Cat#: XF-P1700) following the manufacturer's instructions, with recombinant protein human matrix metalloproteinase 2 (PreproTech, Cat#:420-02-10UG) as a positive control.

2.6 | ELISA

Serum TNF-α levels in ApoE$^{-/-}$Mep1A$^{+/+}$ and ApoE$^{-/-}$Mep1A$^{-/-}$ mice and TNF-α levels in IgE-treated mast cell supernatant were detected by a commercial TNF-α ELISA Kit (eBioscience, CA, USA, Cat#: 85-88-7324-22) following the manufacturer's instructions. Briefly, 96-well ELISA plates were coated overnight with capture antibody. Serum or cell culture supernatants were added for 2 hr. After a washing step with PBS-Tween 20, the detection antibody was added, followed by the addition of HRP-conjugated streptavidin and 3,3′,5,5′-tetramethylbenzidine. The reaction was stopped with 0.5-M H$_2$SO$_4$, and the absorbance was monitored at 450 nm.

2.7 | Cell culture and small-interfering RNA

RBL-2H3 mast cells were purchased from American Type Culture Collection (Manassas, VA, USA) and cultured in DMEM (Solarbio, China, Cat#: 12100-500) containing 10% FBS, 100 U·ml^{-1} of penicillin, and 100 g·ml^{-1} of streptomycin. RAW264.7 macrophages were purchased from the National Infrastructure of Cell Line Resource and cultured in DMEM. Human s were purchased from the ScienCell Research Laboratories, Inc. (Cat#: 6110, San Diego, CA, USA), and cultured in smooth muscle cell medium (ScienCell) containing 2% FBS, 100 U·ml^{-1} of penicillin, and 100 g·ml^{-1} of streptomycin. For the in vitro experiments, cells were cultured in six-well plates (6 × 10^5 cells per well; NEST, Cat#: 703001) and stimulated with 10 μg·ml^{-1} of IgE (Sigma, Cat#: D8406-.5MG).

To inhibit Mep1A, 100 μmol·L^{-1} of actinonin (Mep1A inhibitor, CAS 13434-13-4, Santa Cruz Biotechnology, USA) was added 1 hr before IgE treatment. To knockdown Mep1A, Mep1A small-small-interfering RNA (siRNA) and control siRNA were purchased from Ambion (Austin, TX, USA, Cat#: 4390771). siRNA transfections were performed according to the manufacturer's protocol. Briefly, RBL-2H3 cells at 80% confluence were transfected with 100-nM siRNA duplexes in 5 μL of Oligofectamine (Invitrogen, Carlsbad, CA, USA, Cat#: 12252011). After 6 hr, the medium was changed.

2.8 | Flow cytometry

Human smooth muscle cell apoptosis was analysed by flow cytometry. Briefly, the cell suspension was filtered, centrifuged, and resuspended. Cells were stained following the protocol of the Annexin V-FITC/PI Apoptosis Detection Kit (Yeasen, China, Cat#: 40302ES50). The data were obtained and analysed using a BD Accuri C6 flow cytometer (BD, USA).

2.9 | Data and analysis

Statistical analysis was undertaken only for studies where each group size was at least $n = 5$. Data are expressed as the mean ± SEM. The declared group size was the number of independent values, and that statistical analysis was done using these independent values. In this study, outliers were included in data analysis and presentation. P value <.05 was considered statistically significant for all tests. The independent samples t-test was performed to compare two groups, and five independent experiments were performed. Two-way or one-way ANOVA with Bonferroni's post hoc test was performed to compare multiple groups. In multigroup studies with parametric variables, post hoc tests were conducted when F in ANOVA achieved the "chosen" necessary level of statistical significance and there was no significant variance inhomogeneity. P value for statistical significance was not varied later in Section 3. The mouse survival rate was assessed using Kaplan–Meier analysis. Due to reducing unwanted variation, we used "fold mean of the controls" to normalize the data of western blotting and RT-PCR statistics. The data and statistical analysis comply with the recommendations of the *British Journal of Pharmacology* on experimental design and analysis in pharmacology (Curtis et al., 2018).

2.10 | Nomenclature of targets and ligands

Key protein targets and ligands in this article are hyperlinked to corresponding entries in http://www.guidetopharmacology.org, the common portal for data from the IUPHAR/BPS Guide to PHARMA-COLOGY (Harding et al., 2018) and are permanently archived in the Concise Guide to PHARMACOLOGY 2019/20 (Alexander et al., 2019).

3 | RESULTS

3.1 | Expression of Mep1A in human and mouse abdominal aortic aneurysm tissues

To ascertain whether Mep1A and Mep1B are expressed in abdominal aortic aneurysm tissue, a well-established Ang II-induced abdominal aortic aneurysm mouse model was used. Two groups were generated: ApoE$^{-/-}$Mep1A$^{+/+}$ (WT) mice treated with Ang II and WT mice treated with PBS. The aortas were harvested from mice with abdominal aortic aneurysm and healthy control mice, and mRNA (Figure 1a) and protein (Figure 1b,c) expression levels of Mep1A and Mep1B were determined. Higher expression of Mep1A, but not Mep1B, was detected in the aortic wall of mice with abdominal aortic aneurysm compared with control mice. Consistently, the immunohistochemistry analysis also revealed that more Mep1A-positive area was shown in abdominal aortic aneurysm tissues (Figure 1d,e). Moreover, during abdominal aortic aneurysm progression, Mep1A expression showed an increasing trend at different time points with the peak of Day 14 (Figure S1C). To further confirm Mep1A expression in abdominal aortic aneurysm tissues, aortas from abdominal aortic aneurysm patients and controls were examined. As shown in Figure 1f–j, Mep1A was also highly expressed in human abdominal aortic aneurysm tissues but not in control aortas. These data together indicate an
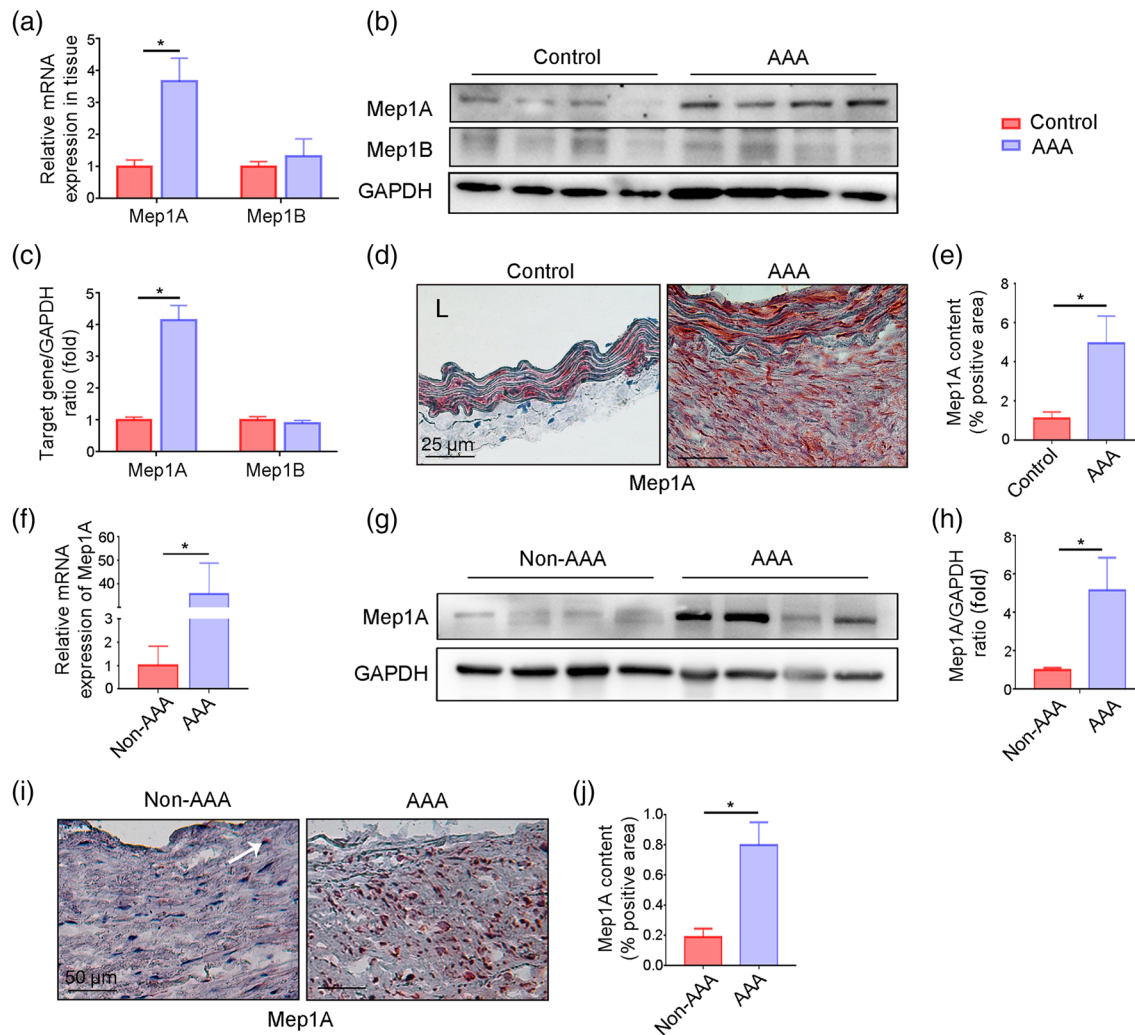
FIGURE 1 Mep1A expression in abdominal aortic aneurysm (AAA) tissue. (a) RT-PCR analysis of Mep1A and Mep1B expression in the arterial wall of the mice (control: $n = 5$, AAA: $n = 6$). (b) Immunoblot analysis of Mep1A and Mep1B expression in arterial walls from mice with normal arteries and those with AAA. (c) Quantification of Mep1A and Mep1B expression in mice by immunoblotting (control: $n = 5$, AAA: $n = 6$). (d) Immunohistochemistry analysis of Mep1A in normal mouse arteries and AAA tissues. (e) The graph presents the percentage of Mep1A-positive area in normal mouse arteries and AAA tissues (control: $n = 5$, AAA: $n = 6$). (f) RT-PCR analysis of Mep1A expression in the arterial wall of human non-AAA arteries ($n = 7$) and AAA tissues ($n = 6$). (g) Representative immunoblot image of Mep1A in human non-AAA arteries and AAA tissues. (h) Quantification of Mep1A expression in human non-AAA ($n = 7$) and AAA tissues ($n = 6$) by immunoblotting. (i) Immunohistochemistry analysis of Mep1A in human non-AAA arteries and AAA tissues. The arrow pointed the Mep1A positive staining area in non-AAA tissues. (j) The graph presents the percentage of Mep1A-positive area in human non-AAA arteries ($n = 7$) and AAA tissues ($n = 6$). Data represent the mean ± SEM. Student's t-test was conducted to examine the differences between group in all data from experimental AAAs. *$P < .05$ was considered statistically significant. L, lumen

increased expression of Mep1A in abdominal aortic aneurysm tissues during abdominal aortic aneurysm progression.

3.2 | Mep1A deficiency decreased Ang II-induced abdominal aortic aneurysm formation

To evaluate the effect of Mep1A deficiency on abdominal aortic aneurysm in our mouse model (WT: ApoE$^{-/-}$Mep1A$^{+/+}$; KO: ApoE$^{-/-}$Mep1A$^{-/-}$), the mortality, morbidity and aortic diameter were measured in the four groups, namely, the WT control, KO control, WT

Ang II and KO Ang II groups. Kaplan–Meier analysis of survival showed that 36.4% of the WT mice died within 28 days of Ang II treatment, whereas only 8.3% of Mep1A KO mice died after Ang II treatment (Figure 2a,b). To more fully elucidate the underlying pathology, we performed necropsy of the deceased mice. As shown in Figure S2A, abdominal aortic aneurysm rupture caused mouse death. Furthermore, the incidence of abdominal aortic aneurysm was lower in KO mice than in WT mice (45.5% vs. 71.4%, Figure 2c). Moreover, the average diameter of the aorta was smaller in KO mice than in WT mice (WT: 1.886 ± 0.216 mm; KO: 1.309 ± 0.105 mm; Figure 2d–f). In addition, systolic and diastolic BPs increased after Ang II treatment
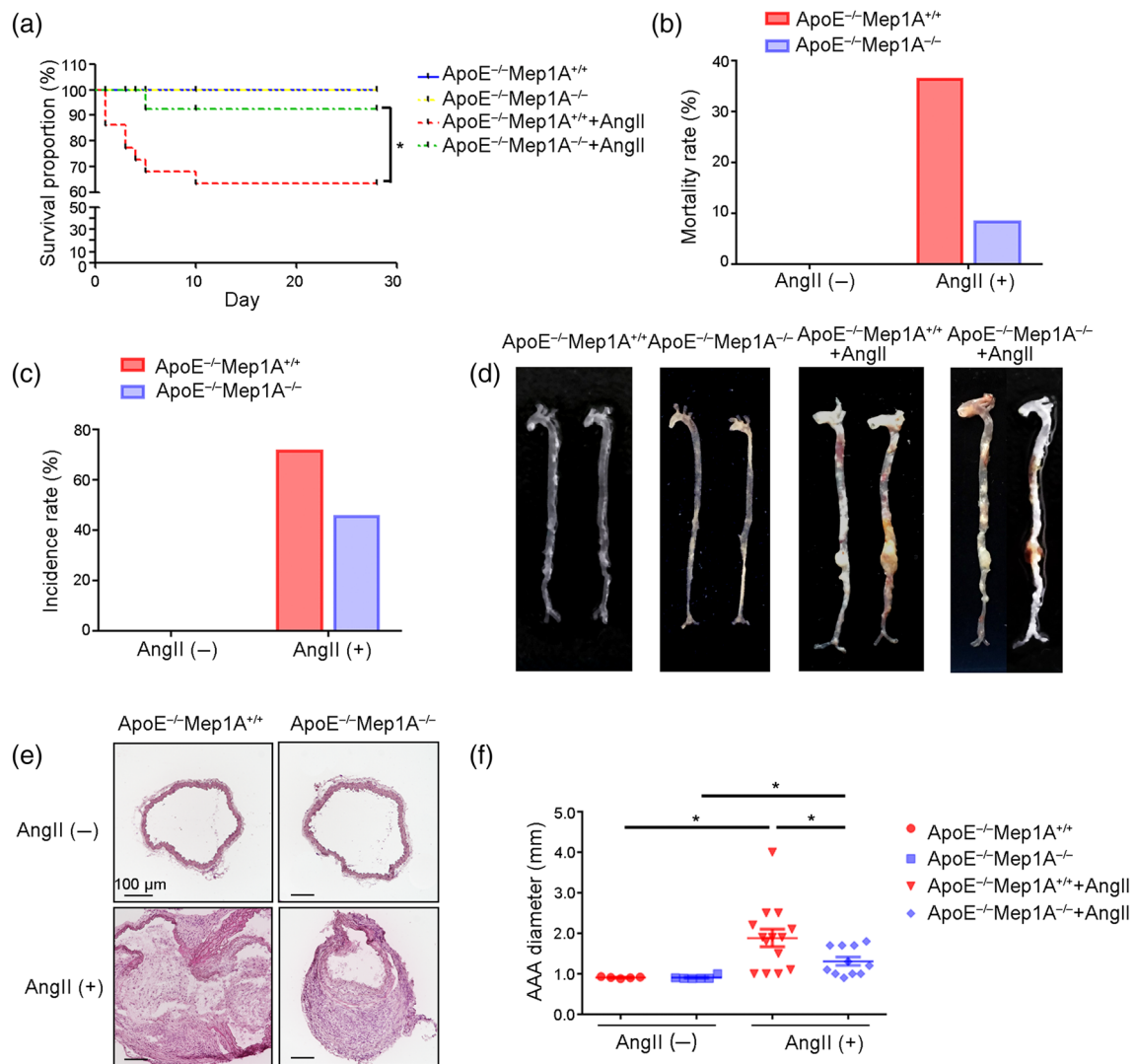
FIGURE 2 Role of Mep1A in Ang II-induced abdominal aortic aneurysm (AAA) in mice. (a) Graph of the survival rates of mice of the indicated genotypes under the experimental conditions. ApoE$^{-/-}$Mep1A$^{+/+}$ mice treated with PBS (n = 5), ApoE$^{-/-}$Mep1A$^{-/-}$ mice treated with PBS (n = 6), ApoE$^{-/-}$Mep1A$^{+/+}$ mice treated with Ang II (n = 14) and ApoE$^{-/-}$Mep1A$^{-/-}$ mice treated with Ang II (n = 11). (b) The AAA-associated mortality rate in ApoE$^{-/-}$Mep1A$^{-/-}$ and ApoE$^{-/-}$Mep1A$^{+/+}$ mice on the 28th day after Ang II infusion. (c) The incidence rate of AAA in ApoE$^{-/-}$Mep1A$^{-/-}$ and ApoE$^{-/-}$Mep1A$^{+/+}$ mice on the 28th day after Ang II infusion. (d) Representative images of whole aortas. (e) Representative images of HE staining of abdominal aortas. (f) Quantification of AAA diameter (mm). Mouse survival rates were determined using Kaplan–Meier analysis, and the statistical significance of differences among groups was ascertained. Two-way ANOVA was conducted to examine the differences among groups in other data from experimental AAAs. Data represent the mean ± SEM. *P <.05 was considered statistically significant

(Figure S2B), but there was no difference between the WT and KO mice. These data suggest that Mep1A can mediate abdominal aortic aneurysm formation and stability.

3.3 | Mep1A deficiency prevented Ang II-induced elastic lamina degradation and apoptosis

To further explore how Mep1A affects vessel wall remodelling and stability, immunostaining of abdominal aortic aneurysm tissues was performed. The elastic lamina was more frequently disrupted and degraded in WT mice than in KO mice. A semi-quantitative analysis of elastin lamina degradation showed that Mep1A deficiency inhibited

elastin lamina degradation after Ang II treatment (Figure 3a,b). It has been reported that both collagen and elastin are substrates of matrix metalloproteinases (van Vlijmen-van Keulen, Pals, & Rauwerda, 2002) and genetic and pharmacological inhibition of matrix metalloproteinases, especially **matrix metalloproteinase 2** (MMP2), suppresses aneurysm formation (Manning, Cassis, & Daugherty, 2003; Thompson & Baxter, 1999). Therefore, we next investigated whether matrix metalloproteinase 2 is involved in Mep1A-mediated abdominal aortic aneurysm formation. Our quantitative analysis of immunostaining data showed that matrix metalloproteinase 2 expression was significantly reduced in KO mice compared with WT mice (Figure 3c, d). Moreover, matrix metalloproteinase 2 mRNA and protein levels in abdominal aortic aneurysm tissues were consistent with the staining
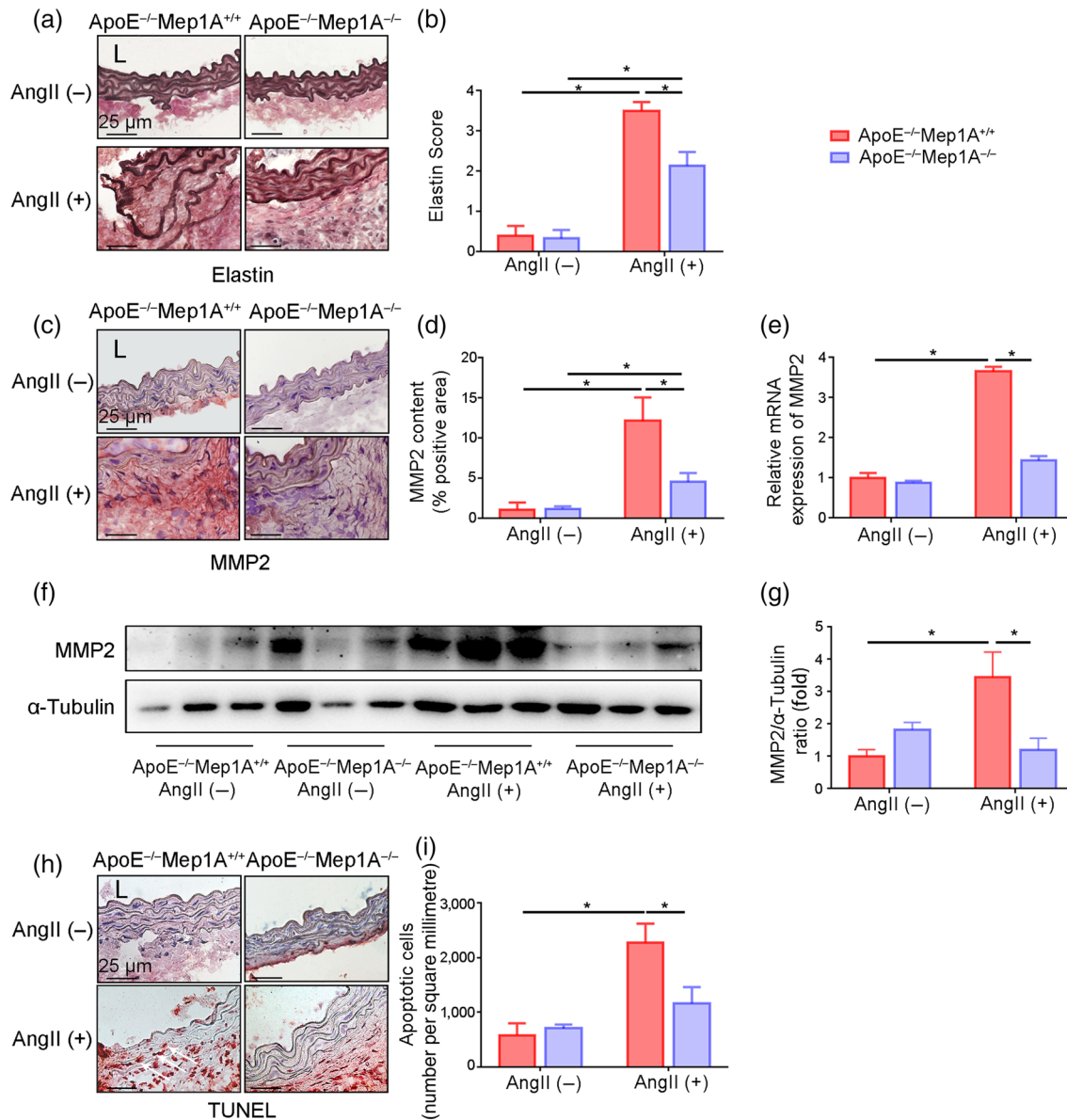
FIGURE 3 Mep1A deficiency inhibited elastic degradation and apoptosis in mice. (a) Staining for elastin to examine the degree of Ang II-induced medial elastin fragmentation in the mouse arterial wall of indicated groups. Elastin staining is indicated by the darkest colour. (b) Quantification of the elastin score. (c) Representative images of the immunohistochemical analysis of matrix metalloproteinase 2 (MMP2) in the mouse arterial wall. (d) The bar graphs show the percentage of MMP2-positive area by immunohistochemistry. (e) RT-PCR was used to measure MMP2 expression in the mouse arterial wall. (f) Representative immunoblotting image of MMP2 expression in the mouse arterial wall or AAA tissue. (g) Quantification of MMP2 expression by immunoblotting. (h) Representative images showing TUNEL staining (red) of apoptotic cells in the mouse arterial wall of the same groups as in (a). (i) Quantification of apoptotic cells in aortas. Data represent the mean ± SEM. Groups: ApoE$^{-/-}$Mep1A$^{+/+}$ mice treated with PBS ($n = 5$), ApoE$^{-/-}$Mep1A$^{-/-}$ mice treated with PBS ($n = 6$), ApoE$^{-/-}$Mep1A$^{+/+}$ mice treated with Ang II ($n = 5$), and ApoE$^{-/-}$Mep1A$^{-/-}$ mice treated with Ang II ($n = 6$). Two-way ANOVA was conducted to examine the statistical significance of differences among groups in all data from experimental AAAs. $^*P < .05$ was considered statistically significant. L, lumen

results (Figure 3e–g). As apoptosis is vital for pathological remodelling of the vessel wall, apoptosis of cells in the aortic wall of our mouse model was also examined. In our statistical analysis of TUNEL staining, the number of apoptotic cells in abdominal aortic aneurysm tissues was markedly lower in KO mice than in WT mice (1,158 vs. 2,272 cells·mm^{-2}, Figure 3h,i). These data suggest that Mep1A deficiency may inhibit abdominal aortic aneurysm formation by regulating elastin degradation.

## 3.4 | Mep1A regulated inflammatory cell infiltration in vivo

Mep1A has been reported to be crucial in inflammation, neurodegeneration, cancer, and fibrosis (Jefferson et al., 2013). Inflammation is involved in abdominal aortic aneurysm instability, especially in elastin lamina degradation (Jalalzadeh et al., 2016; Kaneko et al., 2011; Kothapalli & Ramamurthi, 2010). To evaluate the effect

of Mep1A deficiency on Ang II-induced vascular inflammation, we assessed the infiltration of several types of inflammatory cells. As shown in Figure 4a,b, the expression of the mast cell marker tryptase in the aneurysm was significantly decreased in KO mice compared with WT mice, indicating that aneurysm formation might be regulated by Mep1A expressed by mast cells. Furthermore, the number of macrophages in the aortic wall was markedly lower in KO mice (Figure 4c, d), suggesting the attenuation of a Mep1A-induced inflammatory response. Moreover, the number of MHC-II-positive cells was significantly lower in KO mice than in WT mice (Figure 4e,f). The T cell marker CD4+ also tended to reduce in aneurysm tissue from KO mice

but this was not statistically significant (Figure 4g,h). These data indicate that Mep1A may regulate inflammation in abdominal aortic aneurysm

3.5 | Mep1A mediated TNF-α expression in mast cells

We next examine which cells express Mep1A in abdominal aortic aneurysm progression. As shown in Figure 5a,b, Mep1A was highly expressed in mast cells, but not endothelial cells and smooth
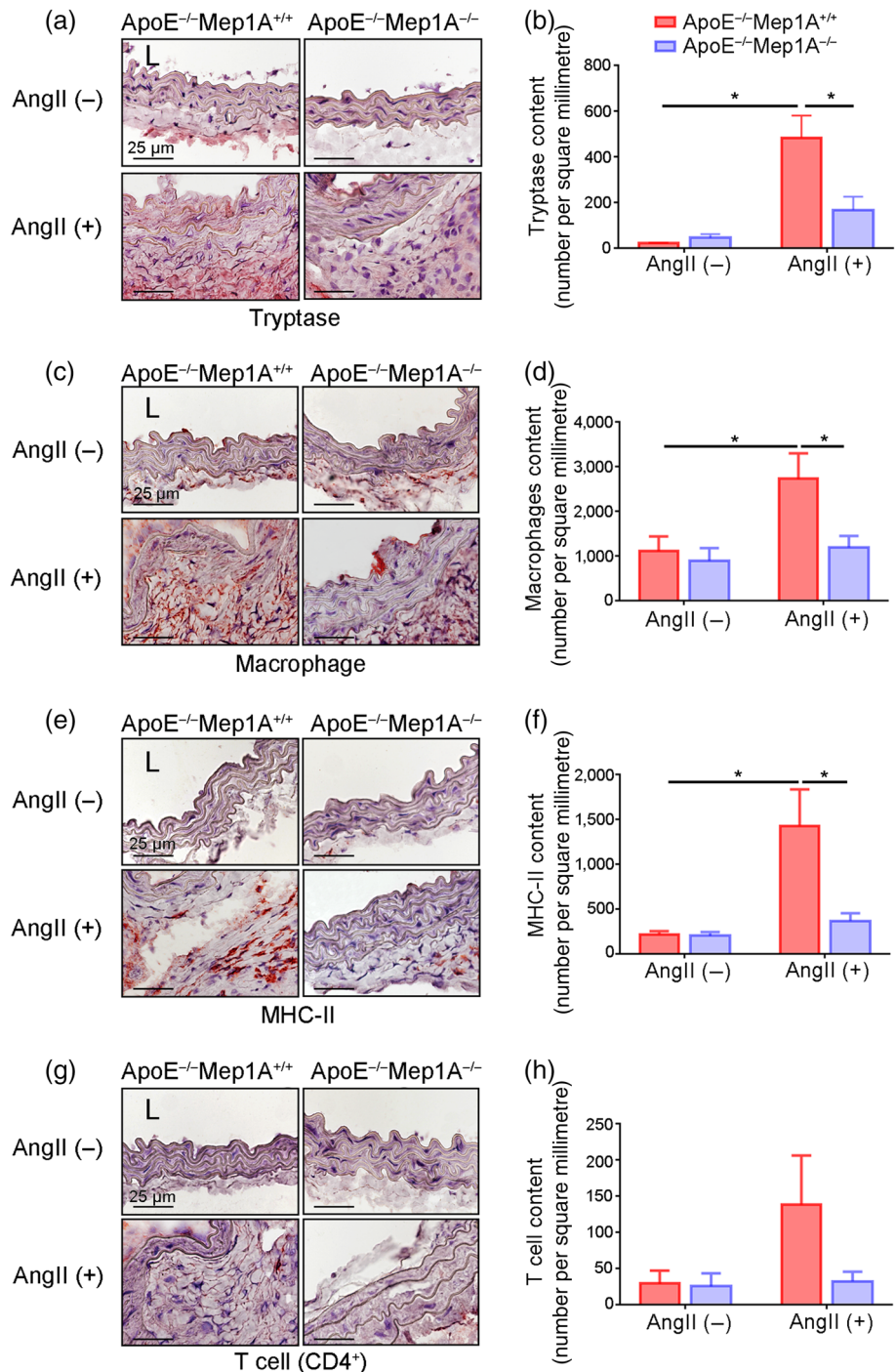
FIGURE 4 Role of Mep1A in inflammation in abdominal aortic aneurysm (AAA). Representative images of the immunohistochemical analysis of (a) tryptase-positive cells, (c) macrophages, (e) MHC-II-positive cells, and (g) CD4+ T cells in the mouse arterial wall. Immunohistochemical analysis of (b) tryptase-positive cells, (d) macrophages, (f) MHC-II-positive cells and (h) CD4+ T cells in the arterial walls of the experimental mice of the indicated groups. The bar graphs present the positive cells per square millimetre. Data represent the mean ± SEM. Groups: ApoE−/−Mep1A+/+ mice treated with PBS (n = 5), ApoE−/−Mep1A−/− mice treated with PBS (n = 6), ApoE−/−Mep1A+/+ mice treated with Ang II (n = 5) and ApoE−/−Mep1A−/− mice treated with Ang II (n = 6). Two-way ANOVA was conducted to examine the differences among groups in all data from experimental AAAs. *P <.05 was considered statistically significant. L, lumen
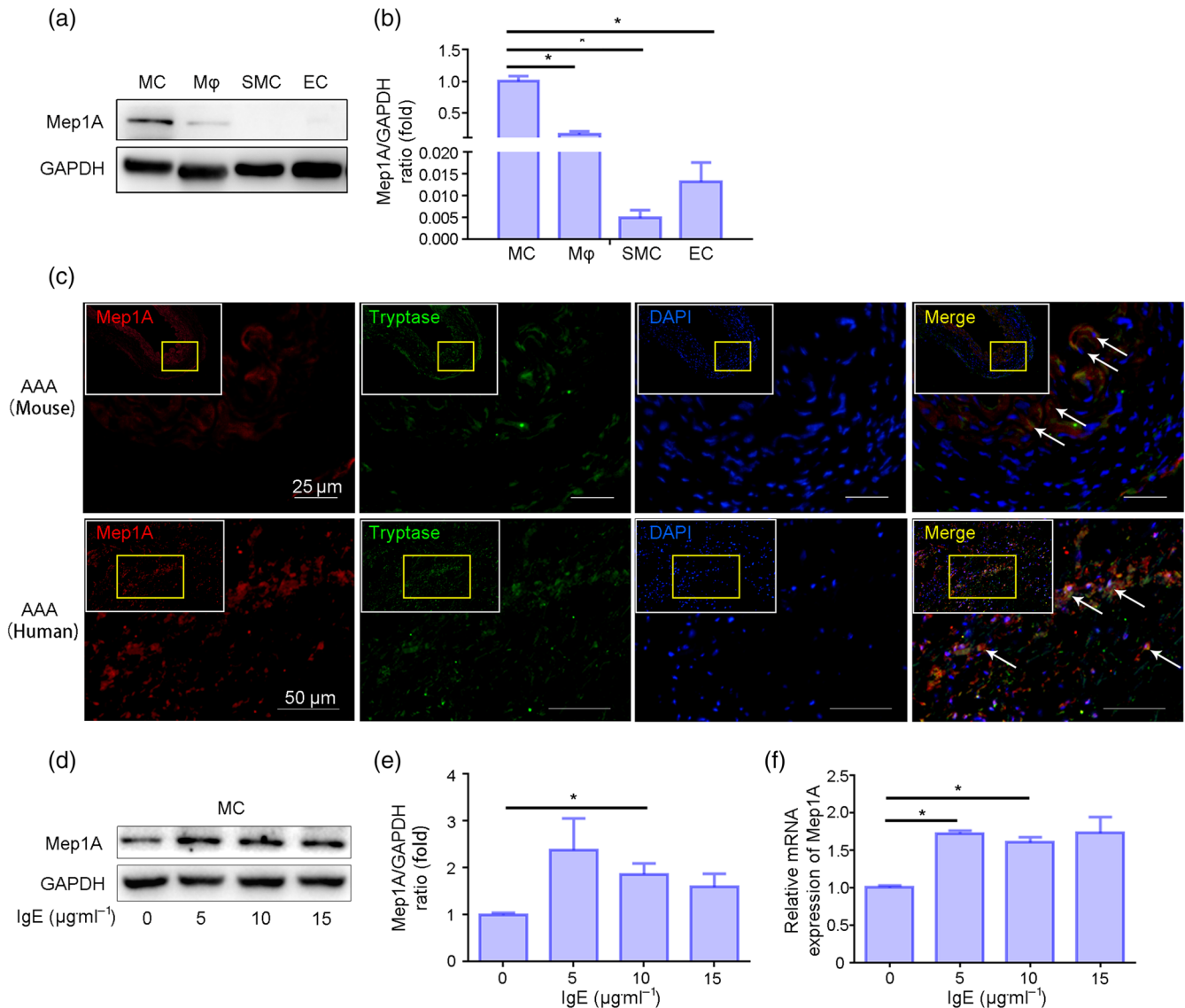
FIGURE 5 IgE up-regulated Mep1A expression in mast cells (MCs). (a) Immunoblot analysis of basal Mep1A expression in the indicated cells including mast cells, macrophages (Mφ), smooth muscle cells (smooth muscle cell) and endothelial cells (ECs). (b) Quantification of Mep1A expression in the indicated cells by immunoblotting. (c) Immunofluorescence staining of Mep1A and tryptase (mast cell marker). Mep1A: red, tryptase: green, DAPI: blue. (d) Immunoblot analysis of Mep1A expression in MCs treated with IgE at the indicated doses. (e) Quantification of immunoblotting results of Mep1A expression in MCs treated with IgE. (f) RT-PCR analysis of Mep1A expression in MCs treated with the indicated doses of IgE. Data are presented as the mean ± SEM of five independent experiments. One-way ANOVA was conducted to examine the differences among groups for all data. *P <.05 was considered statistically significant

muscle cells at basal level, besides macrophages that was reported to express Mep1A (Gao et al., 2009). To further confirm these results in vivo, the immunofluorescence staining was performed in both mouse and human abdominal aortic aneurysm tissue. We found that Mep1A is mainly co-localized in mast cells (Figure 5c), but not in macrophages (Figure S3A), endothelial cells (Figure S3B) and SM smooth muscle cells (Figure S3C). To identify the dynamic changes of Mep1A in mast cells during abdominal aortic aneurysm development, we next stained the abdominal aortic aneurysm tissue after Ang II infusion at Days 0, 3, 7, 14 and 28. The results showed that Mep1A-producing mast cell infiltration tended to increase over time in vivo (Figure S3D), suggesting that Mep1A

expression in Ang II-induced AAA was mainly originating form MCs. Additionally, our previous study had demonstrated that plasma IgE (a well-known mast cell activator) levels are significantly increased in both abdominal aortic aneurysm patients and abdominal aortic aneurysm mice (Wang et al., 2014). Consistently with this, we also found increased IgE levels in abdominal aortic aneurysm mice compared with control (Figure S2C). In addition, mast cells were considered as the main effector cells of IgE (Frossi, De Carli, & Pucillo, 2004). Therefore, we used IgE to stimulate mast cells in vitro to imitate the in vivo environment. We found that IgE up-regulated Mep1A expression in mast cells at both the protein (Figure 5d,e) and mRNA levels (Figure 5f).

Gao and Si (2010) reported that Mep1A promotes the secretion of the inflammatory factors TNF-α and IL-1β from peripheral blood mononuclear cells. We next examined TNF-α and IL-1β secretion by mast cells in response to IgE (10 μg·ml^{-1}, 24 hr). As shown in Figure 6a,b, TNF-α levels increased at both the mRNA and protein levels in IgE-treated mast cells, while IL-1β was unchanged exploratorily (Figure S4A). To further confirm the in vitro results, we examined TNF-α expression in vivo, which was significantly inhibited in KO mice compared to WT mice treated with Ang II (Figure 6c,d). TNF-α mRNA levels were also markedly reduced in aortic tissue (Figure 6e). Furthermore, serum TNF-α levels were lower in KO mice than in WT mice (79.77 ± 1.36 vs. 91.41 ± 4.86 pg·ml^{-1}, Figure 6f).

To determine whether Mep1A mediates IgE-induced TNF-α expression, mast cells were transfected with Mep1A siRNA (100 nM). The knockdown of Mep1A was confirmed by both western blotting and RT-PCR (Figure 6g–i). Mep1A knockdown resulted in a pronounced inhibition of TNF-α expression in IgE-treated mast cells (Figure 6j,k). Moreover, actinonin, a Mep1A inhibitor, induced the same result as siRNA transfection with TNF-α expression, dramatically reducing both the mRNA and protein levels in IgE-treated mast cells (Figure 6l,m). These results indicate that Mep1A is involved in TNF-α secretion from mast cells.

3.6 | TNF-α secretion by mast cells promoted matrix metalloproteinase 2 expression in smooth muscle cells (SMCs) and smooth muscle cell apoptosis

To examine whether TNF-α secreted by mast cells induces matrix metalloproteinase expression in smooth muscle cells, the supernatant from IgE-treated (10 μg·ml^{-1}) mast cells was divided into two equal aliquots; supernatant A and supernatant B. IgG was added to supernatant A as a control, and TNF-α antibody was used to deplete TNF-α in supernatant B (Figure 7a). The removal of TNF-α from supernatant B was confirmed by ELISA (Figure 7b). Then, smooth muscle cells were treated with supernatants A and B. As shown, matrix metalloproteinase 2 expression (Figure 7c,d) and activity (Figure S4B) were significantly increased in smooth muscle cells treated with supernatant A (without TNF-α depletion) but not in those treated with supernatant B (with TNF-α depletion). These data indicated that IgE-induced mast cell-producing high TNF-α, up-regulated matrix metalloproteinase 2 expression and activity in smooth muscle cells.

Similarly, the levels of cleaved caspase-3, an apoptotic cell marker, were significantly increased in only smooth muscle cells treated with supernatant A compared with the control (Figure 7e,f). These results were further verified by flow cytometry analysis (Figure 7g). The apoptosis of smooth muscle cells treated with supernatant B was lower than that of smooth muscle cells cultured in supernatant A (Figure 7h). These data suggest that Mep1A may promote TNF-α secretion by mast cells, which induces matrix metalloproteinase 2 expression in smooth muscle cells and smooth muscle cell apoptosis, thus enhancing abdominal aortic aneurysm formation and rupture.

4 | DISCUSSION

The present study demonstrated that Mep1A deficiency reduced the formation of Ang II-induced abdominal aortic aneurysm and decreased the mortality in mice. Mep1A was robustly expressed and mediated IgE-induced TNF-α expression in mast cells. TNF-α secreted by mast cells enhanced matrix metalloproteinase 2 expression in smooth muscle cells and promoted smooth muscle cell apoptosis, subsequently leading to elastic lamina degradation, abdominal aortic aneurysm formation and eventual death. Mep1A deletion markedly reversed the extensive proteolysis of matrix proteins, smooth muscle cell apoptosis and inflammatory cell accumulation. These results suggest the importance of Mep1A expression in the development of abdominal aortic aneurysm. Knocking out Mep1A might be crucial in preventing abdominal aortic aneurysm rupture.

In our abdominal aortic aneurysm study, Mep1A expression was mainly in mast cells instead of macrophages, smooth muscle cells and endothelial cells (Figure 5c and Figure S3A–C). For further cellular mechanism study, IgE instead of Ang II was used to stimulate mast cells, because mast cells do not express the angiotensin receptors as demonstrated in Figure S4C. The role of IgE in abdominal aortic aneurysm pathogenesis has been previously demonstrated (Wang et al., 2014). IgE promotes abdominal aortic aneurysm formation by activating inflammatory cells, such as macrophages, mast cells and CD4$^+$ T cells in the aortic wall (Liu et al., 2016; Wang et al., 2014). Neutralizing plasma IgE with the IgE antibody may prevent abdominal aortic aneurysm formation (Wang et al., 2014). The present study demonstrates that mast cells expressed Mep1A can be a possible mechanism by which IgE mediates abdominal aortic aneurysm formation.

Meprin was reported to mediate Collagen I and III degradation (Prox, Arnold, & Becker-Pauly, 2015). Mep1A and Mep1B can remove both C-propeptides and N-propeptides, thereby releasing mature Collagen I (Broder et al., 2013), but procollagen I maturation hydrolysed by Mep1B is more efficient (Broder et al., 2013). Moreover, Rao et al. (2015) reported that collagens I and III mainly contribute to the occurrence of intraluminal thrombus during abdominal aortic aneurysm, but few reports have focused on how the collagen family promotes abdominal aortic aneurysm occurrence and development. We detected collagen I mRNA and protein in animal tissues but found no difference between Ang II-infused WT and KO mice (Figure S5A–E), suggesting that Mep1A might regulate abdominal aortic aneurysm formation but it is not mediated by collagen. Nevertheless, it has been shown that meprin plays important roles in inducing inflammation by activating cytokines, such as IL-1β, TNF-α and endothelin (Gao & Si, 2010), which may contribute to atherosclerosis (Gao et al., 2009). Our current data demonstrated that Mep1A also influence abdominal aortic aneurysm formation by regulating TNF-α expression, suggesting that Mep1A may be involved in vascular diseases by regulating inflammation.

TNF-α is an important cytokine found in the inflamed aortic wall of abdominal aortic aneurysm tissue. Manning et al. (2003) reported that TNF-α expression is increased in aneurysms at both the mRNA
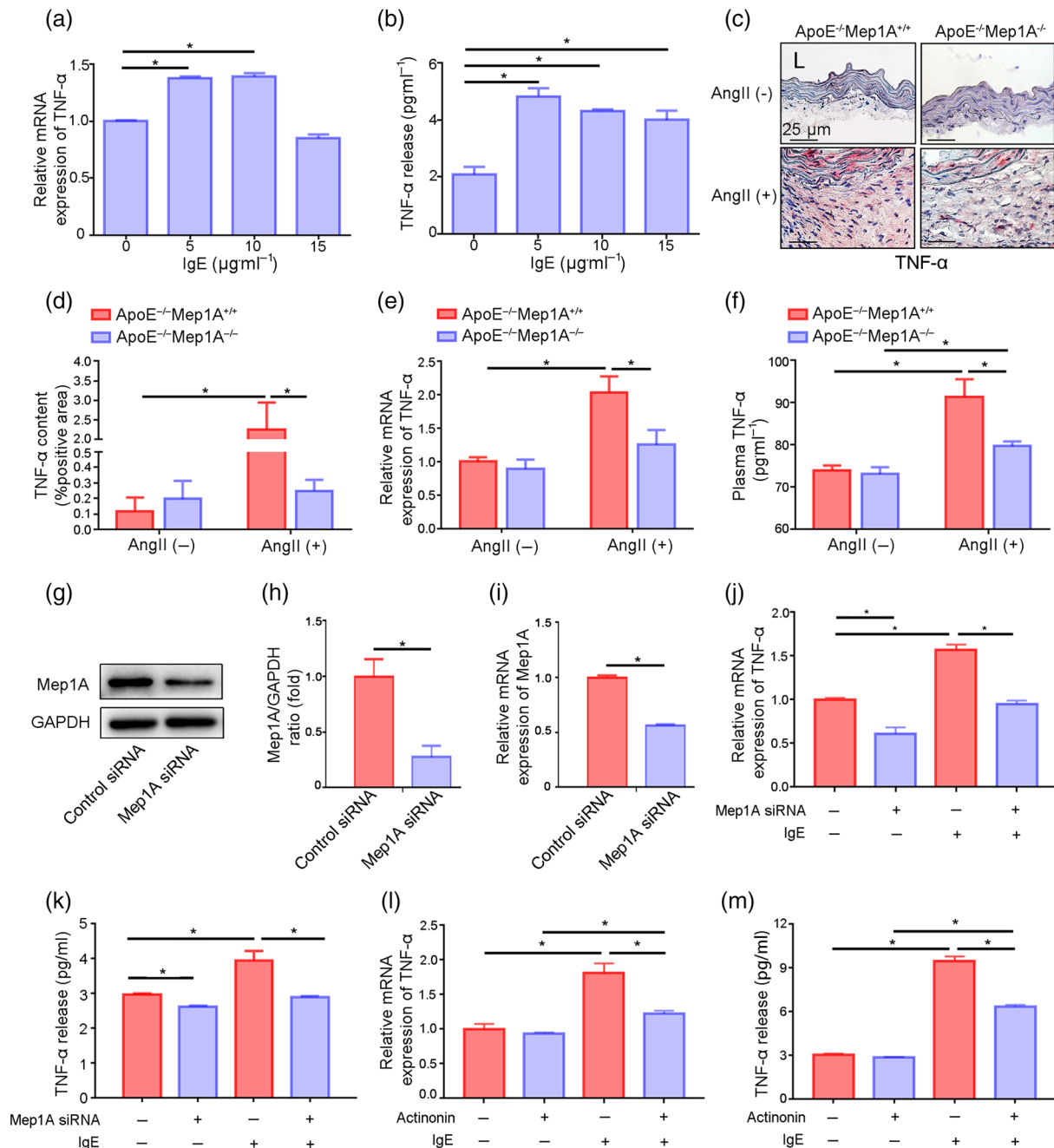
FIGURE 6 Mep1A mediated TNF-α expression in vitro and in vivo. (a) RT-PCR analysis of TNF-α mRNA expression in mast cells (MCs) treated with IgE at the indicated doses. (b) ELISA analyses of TNF-α levels in the supernatants of MCs treated with IgE at the indicated doses. (c) Representative images showing TNF-α staining (red) in the arterial wall of mice of the four groups. (d) Quantification of the immunohistochemical analysis showing the percentage of TNF-α-positive area. (e) RT-PCR analysis of TNF-α mRNA expression in normal arteries and AAA tissues of mice of the indicated groups. (f) ELISA analysis of plasma TNF-α levels in normal and AAA mice of the indicated groups. (g) Immunoblot analysis of Mep1A expression in MCs transfected with Mep1A siRNA (100 nM) or control scrambled siRNA (100 nM). (h) Relative quantification of Mep1A expression. (i) RT-PCR analysis of Mep1A expression in MCs. (j) RT-PCR analysis of TNF-α expression in MCs. (k) ELISA analysis of TNF-α levels in the supernatants of MCs treated as indicated. (l) RT-PCR analysis of TNF-α expression in MCs treated with actinonin (100 μmol·L^{-1}), a Mep1A inhibitor, and IgE (10 μg·ml^{-1}). (m) ELISA analysis of TNF-α levels in the supernatants of MCs treated with actinonin (100 μmol·L^{-1}) and IgE (10 μg·ml^{-1}). Data are presented as the mean ± SEM of five independent experiments in (a), (b), and (h)–(m). Groups in (d)–(f): ApoE$^{-/-}$Mep1A$^{+/+}$ mice treated with PBS ($n = 5$), ApoE$^{-/-}$Mep1A$^{-/-}$ mice treated with PBS ($n = 6$), ApoE$^{-/-}$Mep1A$^{+/+}$ mice treated with Ang II ($n = 5$), and ApoE$^{-/-}$Mep1A$^{-/-}$ mice treated with Ang II ($n = 6$). One-way ANOVA was conducted to examine the differences among groups in (a) and (b). Two-way ANOVA was conducted to examine the differences among groups in (d)–(f) and (j)–(m). Student's t-test was used to examine the differences between groups in (h) and (i). *$P < .05$ was considered statistically significant. L, lumen
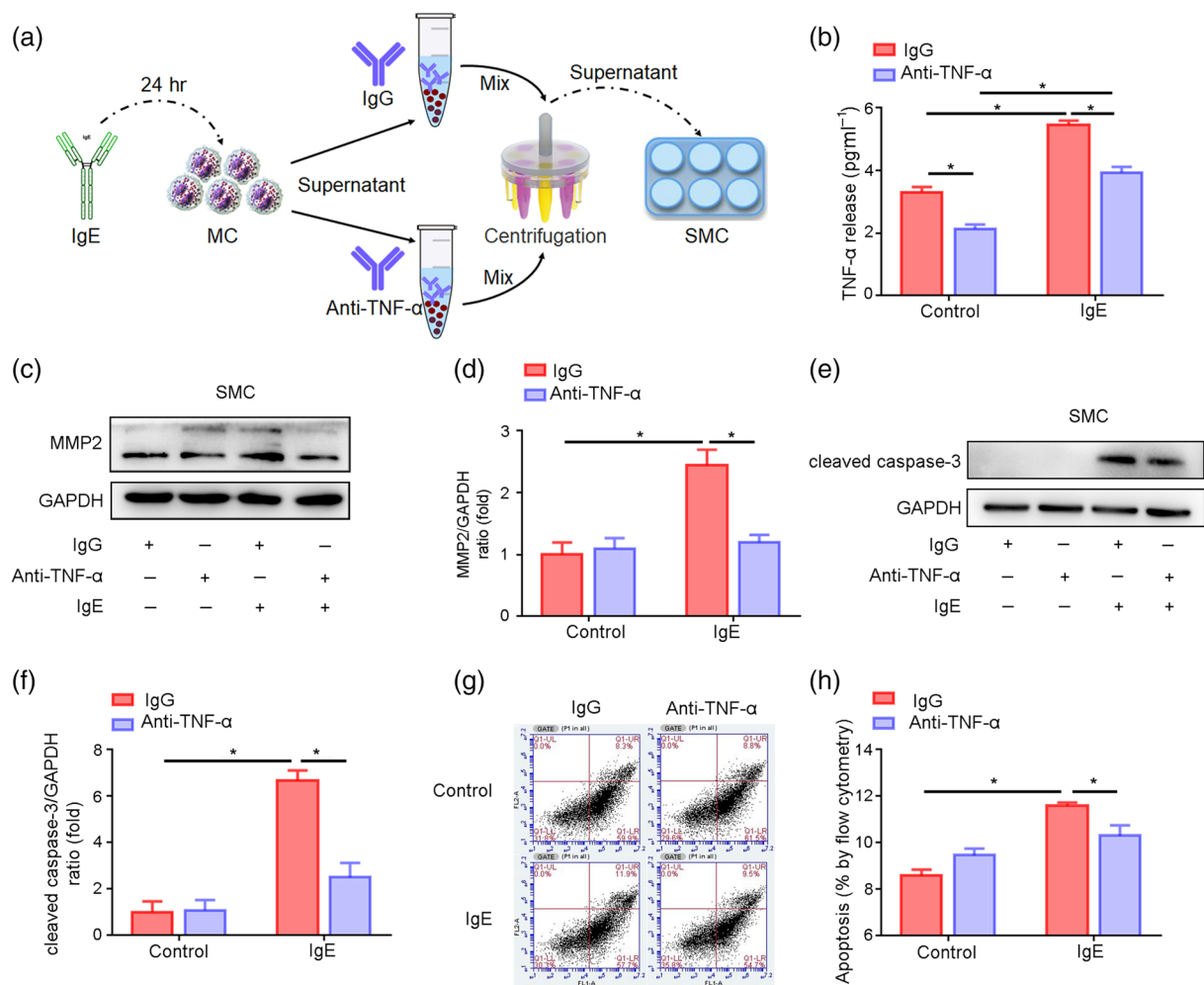
FIGURE 7   TNF-α promoted the expression of matrix metalloproteinase 2 (MMP2) and apoptosis in smooth muscle cells (SMCs). (a) The model of an in vitro experiment to explore the effect of TNF-α secreted by mast cell (MCs) on SMCs. (b) ELISA to detect TNF-α in MC supernatant treated with the antibodies as indicated. (c) Immunoblot to detect the expression of MMP2 in SMCs treated with the indicated supernatant. (d) Quantitative analysis of MMP2 protein levels by immunoblotting. (e) Immunoblot to detect the expression of cleaved caspase-3 in SMCs treated with the indicated supernatant. (f) Quantitative analysis of cleaved caspase-3 expression by immunoblotting. (g) Flow cytometric analysis to measure apoptotic SMCs stained with annexin V/PI. (h) Quantitative illustration of the total (early and late) apoptosis rates of the SMCs under the indicated treatments. Data are the mean ± SEM of five independent experiments. Two-way ANOVA was conducted to examine the statistical difference. *P value <.05 was considered statistically significant

and protein levels. Additionally, TNF-α-deficient mice are resistant to aneurysm formation because macrophage infiltration and matrix metalloproteinase 2 expression are attenuated. These data suggest an important role for TNF-α in regulating aortic inflammation and remodelling. In previous studies, TNF-α has been reported to be produced by macrophages and mast cells (Hsieh et al., 2007; Piliponsky et al., 2012; Romo-Lozano, Hernandez-Hernandez, & Salinas, 2014; Yamamoto et al., 2008). Here, we showed that Mep1A mediated IgE-induced TNF-α secretion in mast cells, which contributed to abdominal aortic aneurysm formation. Deficiency of Mep1A on mast cells significantly decreased TNF-α, leading to the reduction of abdominal aortic aneurysms. In our studies, it was by mast cells that Mep1A is most likely to regulate the expression of TNF-α, as there was very much less expression of Mep1A in macrophages compared with that in mast cells (Figures 5a–c and S3A). Whether the function and origin

of TNF-α is different in diverse abdominal aortic aneurysm development model needs to be further investigated. Hence, our study has shown that Ang II-induced IgE stimulates the production of TNF-α in mast cells, which participated in aortic inflammation and abdominal aortic aneurysm formation.

Mep1A inhibition in vitro with Mep1A siRNA or actinonin (Mep1A inhibitor) actually reduced TNF-α expression, illustrating that TNF-α secretion is dependent on Mep1A. Actinonin, a Mep1A inhibitor, is produced by *Streptomyces sp.* ATCC 14903 (Umezawa et al., 1985). The inhibitory activity of actinonin relies on various metalloproteinases and peptide deformylase (Chen et al., 2000). Actinonin-mediated inhibition of peptide deformylase has antimicrobial effects against gram-positive bacteria. GSK1322322, a lead compound derivative of actinonin, has been tested in a phase II clinical trial for antibacterial activity (Corey et al., 2014). Actinonin-mediated

Mep1A inhibition was used to reduce atherosclerosis in mice by down-regulating IL-1β and TNF-α (Gao & Si, 2010). In our study, actinonin and Mep1A siRNA showed the same function in vitro. Mep1A inhibition could protect aortas from abdominal aortic aneurysm s.

In conclusion, the findings of our study provide novel insight suggesting that Mep1A in mast cells may aggravate cardiovascular diseases. Therefore, a targeted inhibitor of Mep1A may become an effective therapy for cardiovascular diseases such as abdominal aortic aneurysm in the future.

AUTHOR CONTRIBUTIONS

R.G. and D.L. performed the animal experiments; R.G., D.L. and B.L. contributed to writing the manuscript; R.G. organized the figures; W.G. performed the cell experiments; W.G. contributed to the staining experiments; B.L. revised the language of the manuscript; J.W. and Y.Z. contributed to the study design; and J.W. and P.G. provided financial support.

CONFLICT OF INTEREST

The authors declare no conflicts of interest.

DECLARATION OF TRANSPARENCY AND SCIENTIFIC RIGOUR

This declaration acknowledges that this paper adheres to the principles for transparent reporting and scientific rigour of preclinical research as stated in the BJP guidelines for Design & Analysis, Immunoblotting and Immunochemistry and Animal Experimentation and as recommended by funding agencies, publishers and other organisations engaged with supporting research.

ORCID

Jing Wang https://orcid.org/0000-0003-2410-5408

REFERENCES

Alexander, S. P., Kelly, E., Mathie, A., Peters, J. A., Veale, E. L., Armstrong, J. F., et al. (2019). The Concise Guide to Pharmacology 2019/20: Introduction and other protein targets. *British Journal of Pharmacology*, *176*, S1–S20. https://doi.org/10.1111/bph.14747

Alexander, S. P. H., Roberts, R. E., Broughton, B. R. S., Sobey, C. G., George, C. H., Stanford, S. C., ... Ahluwalia, A. (2018). Goals and practicalities of immunoblotting and immunohistochemistry: A guide for submission to the British Journal of Pharmacology. *British Journal of Pharmacology*, *175*, 407–411. https://doi.org/10.1111/bph.14112

Banerjee, S., Oneda, B., Yap, L. M., Jewell, D. P., Matters, G. L., Fitzpatrick, L. R., ... Bond, J. S. (2009). MEP1A allele for meprin A metalloprotease is a susceptibility gene for inflammatory bowel disease. *Mucosal Immunology*, *2*, 220–231. https://doi.org/10.1038/mi.2009.3

Bertenshaw, G. P., Norcum, M. T., & Bond, J. S. (2003). Structure of homo- and hetero-oligomeric meprin metalloproteases. Dimers, tetramers, and high molecular mass multimers. *The Journal of Biological Chemistry*, *278*, 2522–2532. https://doi.org/10.1074/jbc.M208808200

Broder, C., Arnold, P., Vadon-Le Goff, S., Konerding, M. A., Bahr, K., Muller, S., ... Hulmes, D. J. (2013). Metalloproteases meprin α and meprin β are C- and N-procollagen proteinases important for collagen assembly and tensile strength. *Proceedings of the National Academy of Sciences of the United States of America*, *110*, 14219–14224. https://doi.org/10.1073/pnas.1305464110

Chen, D. Z., Patel, D. V., Hackbarth, C. J., Wang, W., Dreyer, G., Young, D. C., ... Yuan, Z. (2000). Actinonin, a naturally occurring antibacterial agent, is a potent deformylase inhibitor. *Biochemistry*, *39*, 1256–1262. https://doi.org/10.1021/bi992245y

Corey, R., Naderer, O. J., O'Riordan, W. D., Dumont, E., Jones, L. S., Kurtinecz, M., & Zhu, J. Z. (2014). Safety, tolerability, and efficacy of GSK1322322 in the treatment of acute bacterial skin and skin structure infections. *Antimicrobial Agents and Chemotherapy*, *58*, 6518–6527. https://doi.org/10.1128/AAC.03360-14

Curtis, M. J., Alexander, S., Cirino, G., Docherty, J. R., George, C. H., Giembycz, M. A., ... Ahluwalia, A. (2018). Experimental design and analysis and their reporting II: Updated and simplified guidance for authors and peer reviewers. *British Journal of Pharmacology*, *175*, 987–993. https://doi.org/10.1111/bph.14153

Daugherty, A., Manning, M. W., & Cassis, L. A. (2000). Angiotensin II promotes atherosclerotic lesions and aneurysms in apolipoprotein E-deficient mice. *The Journal of Clinical Investigation*, *105*, 1605–1612. https://doi.org/10.1172/JCI7818

Deckert, V., Kretz, B., Habbout, A., Raghay, K., Labbe, J., Abello, N., ... Lagrost, L. (2013). Development of abdominal aortic aneurysm is decreased in mice with plasma phospholipid transfer protein deficiency. *The American Journal of Pathology*, *183*, 975–986. https://doi.org/10.1016/j.ajpath.2013.05.018

Frossi, B., De Carli, M., & Pucillo, C. (2004). The mast cell: An antenna of the microenvironment that directs the immune response. *Journal of Leukocyte Biology*, *75*, 579–585. https://doi.org/10.1189/jlb.0603275

Gao, P., Guo, R. W., Chen, J. F., Chen, Y., Wang, H., Yu, Y., & Huang, L. (2009). A meprin inhibitor suppresses atherosclerotic plaque formation in ApoE$^{-/-}$ mice. *Atherosclerosis*, *207*, 84–92. https://doi.org/10.1016/j.atherosclerosis.2009.04.036

Gao, P., & Si, L. Y. (2010). Meprin-α metalloproteases enhance lipopolysaccharide-stimulated production of tumour necrosis factor-α and interleukin-1β in peripheral blood mononuclear cells via activation of NF-κB. *Regulatory Peptides*, *160*, 99–105. https://doi.org/10.1016/j.regpep.2009.12.009

Harding, S. D., Sharman, J. L., Faccenda, E., Southan, C., Pawson, A. J., Ireland, S., ... NC-IUPHAR (2018). The IUPHAR/BPS Guide to pharmacology in 2018: Updates and expansion to encompass the new guide to immunopharmacology. *Nucleic Acids Research*, *46*(D1), D1091–d1106. https://doi.org/10.1093/nar/gkx1121

Hsieh, C. J., Hall, K., Ha, T., Li, C., Krishnaswamy, G., & Chi, D. S. (2007). Baicalein inhibits IL-1β- and TNF-α-induced inflammatory cytokine production from human mast cells via regulation of the NF-κB pathway. *Clinical and Molecular Allergy: CMA*, *5*, 5. https://doi.org/10.1186/1476-7961-5-5

Jalalzadeh, H., Indrakusuma, R., Planken, R. N., Legemate, D. A., Koelemay, M. J., & Balm, R. (2016). Inflammation as a predictor of abdominal aortic aneurysm growth and rupture: A systematic review of imaging biomarkers. *European Journal of Vascular and Endovascular Surgery: The Official Journal of the European Society for Vascular Surgery*, *52*, 333–342.

Jefferson, T., Auf dem Keller, U., Bellac, C., Metz, V. V., Broder, C., Hedrich, J., … Becker-Pauly, C. (2013). The substrate degradome of meprin metalloproteases reveals an unexpected proteolytic link between meprin β and ADAM10. *Cellular and Molecular Life Sciences: CMLS*, *70*, 309–333. https://doi.org/10.1007/s00018-012-1106-2

Jones, G. T., Tromp, G., Kuivaniemi, H., Gretarsdottir, S., Baas, A. F., Giusti, B., … Bown, M. J. (2017). Meta-analysis of genome-wide association studies for abdominal aortic aneurysm identifies four new disease-specific risk loci. *Circulation Research*, *120*, 341–353. https://doi.org/10.1161/CIRCRESAHA.116.308765

Kaneko, H., Anzai, T., Horiuchi, K., Kohno, T., Nagai, T., Anzai, A., … Fukuda, K. (2011). Tumor necrosis factor-α converting enzyme is a key mediator of abdominal aortic aneurysm development. *Atherosclerosis*, *218*, 470–478. https://doi.org/10.1016/j.atherosclerosis.2011.06.008

Kilkenny, C., Browne, W., Cuthill, I. C., Emerson, M., Altman, D. G., & Group NCRRGW (2010). Animal research: reporting in vivo experiments: The ARRIVE guidelines. *British Journal of Pharmacology*, *160*, 1577–1579.

Kothapalli, C. R., & Ramamurthi, A. (2010). Induced elastin regeneration by chronically activated smooth muscle cells for targeted aneurysm repair. *Acta Biomaterialia*, *6*, 170–178. https://doi.org/10.1016/j.actbio.2009.06.006

Li, D. Y., Busch, A., Jin, H., Chernogubova, E., Pelisek, J., Karlsson, J., … Maegdefessel, L. (2018). H19 induces abdominal aortic aneurysm development and progression. *Circulation*, *138*, 1551–1568. https://doi.org/10.1161/CIRCULATIONAHA.117.032184

Li, J., Krishna, S. M., & Golledge, J. (2016). The potential role of kallistatin in the development of abdominal aortic aneurysm. *International Journal of Molecular Sciences*, *17*(8), 1312. https://doi.org/10.3390/ijms17081312

Lindberg, S., Zarrouk, M., Holst, J., & Gottsater, A. (2016). Inflammatory markers associated with abdominal aortic aneurysm. *European Cytokine Network*, *27*, 75–80. https://doi.org/10.1684/ecn.2016.0381

Liu, C. L., Wemmelund, H., Wang, Y., Liao, M., Lindholt, J. S., Johnsen, S. P., … Shi, G. P. (2016). Asthma associates with human abdominal aortic aneurysm and rupture. *Arteriosclerosis, Thrombosis, and Vascular Biology*, *36*, 570–578. https://doi.org/10.1161/ATVBAHA.115.306497

Manning, M. W., Cassis, L. A., & Daugherty, A. (2003). Differential effects of doxycycline, a broad-spectrum matrix metalloproteinase inhibitor, on angiotensin II-induced atherosclerosis and abdominal aortic aneurysms. *Arteriosclerosis, Thrombosis, and Vascular Biology*, *23*, 483–488.

McGrath, J. C., & Lilley, E. (2015). Implementing guidelines on reporting research using animals (ARRIVE etc.): New requirements for publication in BJP. *British Journal of Pharmacology*, *172*, 3189–3193. https://doi.org/10.1111/bph.12955

Piliponsky, A. M., Chen, C. C., Rios, E. J., Treuting, P. M., Lahiri, A., Abrink, M., … Galli, S. J. (2012). The chymase mouse mast cell protease 4 degrades TNF, limits inflammation, and promotes survival in a model of sepsis. *The American Journal of Pathology*, *181*, 875–886. https://doi.org/10.1016/j.ajpath.2012.05.013

Prox, J., Arnold, P., & Becker-Pauly, C. (2015). Meprin α and meprin β: Procollagen proteinases in health and disease. *Matrix Biology: Journal of the International Society for Matrix Biology*, *44-46*, 7–13. https://doi.org/10.1016/j.matbio.2015.01.010

Rao, J., Brown, B. N., Weinbaum, J. S., Ofstun, E. L., Makaroun, M. S., Humphrey, J. D., & Vorp, D. A. (2015). Distinct macrophage phenotype and collagen organization within the intraluminal thrombus of abdominal aortic aneurysm. *Journal of Vascular Surgery*, *62*, 585–593. https://doi.org/10.1016/j.jvs.2014.11.086

Romo-Lozano, Y., Hernandez-Hernandez, F., & Salinas, E. (2014). Sporothrix schenckii yeasts induce ERK pathway activation and secretion of IL-6 and TNF-α in rat mast cells, but no degranulation. *Medical Mycology*, *52*, 862–868. https://doi.org/10.1093/mmy/myu055

Sakalihasan, N., Limet, R., & Defawe, O. D. (2005). Abdominal aortic aneurysm. *Lancet*, *365*, 1577–1589. https://doi.org/10.1016/S0140-6736(05)66459-8

Schulte, S., Sun, J., Libby, P., Macfarlane, L., Sun, C., Lopez-Ilasaca, M., … Sukhova, G. K. (2010). Cystatin C deficiency promotes inflammation in angiotensin II-induced abdominal aortic aneurisms in atherosclerotic mice. *The American Journal of Pathology*, *177*, 456–463. https://doi.org/10.2353/ajpath.2010.090381

Shi, G. P., & Lindholt, J. S. (2013). Mast cells in abdominal aortic aneurysms. *Current Vascular Pharmacology*, *11*, 314–326. https://doi.org/10.2174/1570161111311030006

Sun, J., Sukhova, G. K., Yang, M., Wolters, P. J., MacFarlane, L. A., Libby, P., … Shi, G. P. (2007). Mast cells modulate the pathogenesis of elastase-induced abdominal aortic aneurysms in mice. *The Journal of Clinical Investigation*, *117*, 3359–3368. https://doi.org/10.1172/JCI31311

Thompson, R. W., & Baxter, B. T. (1999). MMP inhibition in abdominal aortic aneurysms. *Rationale for a Prospective Randomized Clinical Trial. Annals of the New York Academy of Sciences*, *878*, 159–178. https://doi.org/10.1111/j.1749-6632.1999.tb07682.x

Tsuruda, T., Kato, J., Hatakeyama, K., Kojima, K., Yano, M., Yano, Y., … Kitamura, K. (2008). Adventitial mast cells contribute to pathogenesis in the progression of abdominal aortic aneurysm. *Circulation Research*, *102*, 1368–1377. https://doi.org/10.1161/CIRCRESAHA.108.173682

Umezawa, H., Aoyagi, T., Tanaka, T., Suda, H., Okuyama, A., Naganawa, H., … Takeuchi, T. (1985). Production of actinonin, an inhibitor of aminopeptidase M, by actinomycetes. *The Journal of Antibiotics*, *38*, 1629–1630. https://doi.org/10.7164/antibiotics.38.1629

van Vlijmen-van Keulen, C. J., Pals, G., & Rauwerda, J. A. (2002). Familial abdominal aortic aneurysm: A systematic review of a genetic background. *European Journal of Vascular and Endovascular Surgery: The Official Journal of the European Society for Vascular Surgery*, *24*, 105–116.

Wang, J., Lindholt, J. S., Sukhova, G. K., Shi, M. A., Xia, M., Chen, H., … Shi, G. P. (2014). IgE actions on CD4+ T cells, mast cells, and macrophages participate in the pathogenesis of experimental abdominal aortic aneurysms. *EMBO Molecular Medicine*, *6*, 952–969. https://doi.org/10.15252/emmm.201303811

Yamamoto, N., Kaneko, I., Motohashi, K., Sakagami, H., Adachi, Y., Tokuda, N., … Owada, Y. (2008). Fatty acid-binding protein regulates LPS-induced TNF-α production in mast cells. *Prostaglandins, Leukotrienes, and Essential Fatty Acids*, *79*, 21–26. https://doi.org/10.1016/j.plefa.2008.06.003

Zhang, J., Chen, H., Liu, L., Sun, J., Shi, M. A., Sukhova, G. K., & Shi, G. P. (2012). Chemokine (C-C motif) receptor 2 mediates mast cell migration to abdominal aortic aneurysm lesions in mice. *Cardiovascular Research*, *96*, 543–551. https://doi.org/10.1093/cvr/cvs262

SUPPORTING INFORMATION

Additional supporting information may be found online in the Supporting Information section at the end of this article.